International Journal of Rock Mechanics and Mining Sciences 99 (2017) 39–49

Contents lists available at ScienceDirect

International Journal of Rock Mechanics and Mining Sciences

journal homepage: www.elsevier.com/locate/ijrmms

A comparison of the application of block theory and 3D block-cutting analysis

Qi-Hua Zhang*, Xiu-Li Ding, Ai-Qing Wu

Yangtze River Scientific Research Institute, Wuhan, Hubei 430010, China

ARTICLE INFO

Keywords:
Block theory
3D block-cutting analysis
Support-required block
Progressive failure of blocks

ABSTRACT

In hard rock masses, rock destruction is often manifested in the form of the local failure of the blocks formed due to fracturing. In this paper, we compare the application of block theory and three-dimensional (3D) block-cutting analysis to underground caverns. Using block theory, we can determine both the type of removable block and key block for different excavation surfaces. We can then identify 'support-required' blocks from the key blocks by drawing and analyzing the shapes of the maximum likely blocks (i.e. the largest blocks likely to be formed when the fractures are extended indefinitely in a definite-sized cavern). Subsequently, 3D block-cutting analysis is used to identify all the spatial blocks cut by all the finite-sized fractures in the rock mass region. Based on the geometrical information gathered about each spatial block, we carry out an analysis of the progressive failure of the block system. The simulation results allow us to explore the statistical laws governing the distribution of progressive failure blocks. This is a very important aspect which can be used to determine the spacing and length of the rock bolts required, or to check the design of the intended rock support regime. Overall, if we can understand the shortcomings of classic block theory (due to, for example, the assumptions made) and properly utilize the benefits gained from 3D block-cutting analysis, we can deal with more complicated issues. Thus, we hope to gain a more intensive and extensive understanding of block failure analysis.

1. Introduction

Rock masses are, in general, composed of rock blocks and fractures (including joints, cracks, faults, and other kinds of discontinuity). The fractures divide the rock mass into blocks of various sizes and shapes and may vary greatly in different rock masses. The opening, closing, and shearing of fractures often lead to deformation and instability of the rock mass. Indeed, rock destruction is often a manifestation of local block failure, especially in hard rock masses.

In 1985, Goodman and Shi formally proposed 'block theory'.[1] Inherent in this theory are three assumptions or, should we say, preconditions for the application of the theory in engineering. First, fractures are assumed to be infinite planes. Secondly, the blocks formed by fractures and excavation surface(s) act as rigid bodies. Thirdly, any motion of a block is assumed to be translational in nature, i.e. rotational motion is not considered. According to the theory, the removability and failure mode of a block (under the action of an active resultant force) can be analyzed using geometrical and topological methods. Potentially unstable (or 'key') blocks can be determined by carrying out a comparatively simple mechanical analysis. As a result of the analysis, the support forces required to ensure the stability of the key blocks can be calculated.

Block theory has a *rigorous* mathematical foundation. The foundation and essence of the theory is contained within the theorems and methods it is based upon (the finiteness and removability theorems, the stereographic projection, the vector operation methods, and the analysis of the equilibrium region). Since the theory was first proposed, much theoretical progress has been achieved. Accomplishments include: block stability analysis (which considers the action of complicated forces), simulation of discrete fracture networks and stochastic block analysis,[2–4] statistical analysis of stochastic blocks,[5] block reliability analysis,[6] etc. At the same time, the theory has been widely applied around the world to analyze the local stability of fractured rock masses.

Block theory can determine the joint pyramid (JP) and block types formed by several fracture sets. Fractures are assumed to be infinite and their locations indeterminate. If a block is located on an excavation surface, or has two or more convexly-intersecting excavation surfaces, it is convex. If a block includes two or more concavely-intersecting excavation surfaces, e.g. at the corner or roof of an underground chamber, the block is concave.

Unfortunately, block theory may not always be a suitable approach

* Corresponding author.
E-mail address: zqh7692@163.com (Q.-H. Zhang).

http://dx.doi.org/10.1016/j.ijrmms.2017.09.005
Received 22 March 2017; Received in revised form 10 July 2017; Accepted 19 September 2017

Table 1
The difficulties encountered applying block theory.

Difficulty	Cause of difficulty
It is difficult to determine the volume of the blocks in classic block theory.	Fractures are assumed to be infinite planes.
Multi-plane sliding may occur. Or, failure mode is approximately single-plane sliding, even though it is determined to be double-plane sliding.[6,7]	Blocks are assumed to be rigid bodies; blocks assumed to move via translation.
The exact volume of a block has to be determined in order to consider the effect of cohesion (related to the area of the sliding faces).	Cohesion is not considered in classic block theory.
The stability factor (related to cohesion effect) is not continuous when the sliding mode changes from single- to double-plane.	Cohesion is not considered in classic block theory.
The contours of the friction angle required do not exist in the equilibrium region (Londe) picture.	Cohesion is not considered in classic block theory.

to use in some cases, as presented in Table 1. Such difficulties arise because there are conflicts between the assumptions inherent in block theory and the practical engineering demands required of the intended application.

The orientations, extensions, spacing, and positions of fractures are usually randomly formed in a rock mass and will, therefore, vary significantly. Thus, the geometrical configurations and features of the blocks cut by fractures are likely to be *extremely* complex and hence difficult to characterize. A key issue is to identify all the closed blocks cut by a large number of arbitrarily oriented fractures of finite size. The so-called 'method of 3D block-cutting analysis' has been well studied.[8–14] All the blocks formed by the fractures in a certain domain can be identified using this method. The blocks identified are not just those that are exposed but also those located inside the rock mass. The resulting blocks may be convex or concave and be made up of dozens, or even hundreds, of facets.

When a surface block collapses, the constraints on the inner block(s) adjacent to it will disappear. Thus, the newly-exposed inner block(s) become surface block(s) and may also fail. This phenomenon is called progressive block failure.[8,11–13,15,16] The progressive failure process can be analyzed based on the geometries of the blocks identified by 3D block-cutting analysis.[11,13] The progressive failure blocks can be identified by judging their likelihood of failure via certain modes (single-face sliding, double-face sliding, and lifting) in block theory. Hence, they are potentially unstable blocks. If the fractures of blocks possesses sufficient mechanical strength, the progressive failure blocks may self-stabilize. Otherwise, they are key blocks and will fail without support. Progressive block failure is seldom studied and even the practical application of this failure mode is rarely encountered in the public literature.

In this paper, we compare the application of block theory and 3D block-cutting analysis. We do this by taking excavation of an underground cavern as an example. Using block theory, we can determine the types of both removable and key blocks for different excavation surfaces. Among the key blocks we can then identify the 'support-required' blocks. These are the key blocks that are left after we exclude those which are slender and either cling to the excavation surface or penetrate deep into the rock mass.

When employing block theory, the fractures encountered are usually classified into several sets. Furthermore, fractures are assumed to be infinite in extent and ubiquitous. However, in reality, the fractures are finite and their orientations and locations are usually arbitrarily distributed in the rock mass. In this case, it is difficult to determine the blocks using classic block theory. In contrast, 3D block-cutting analysis can identify all the spatial blocks formed by a collection of fractures whose extensions are finite and orientations and locations arbitrarily-distributed. In this work, we employ 3D block-cutting and progressive failure analyses to study the features of the blocks forming in a cavern which has developed a discrete fracture network (DFN) to a certain degree. The simulation results allow us to find the statistical laws governing the distribution of progressive failure blocks. This is a very important result which can be used to determine the spacing and length of rock blots required to stabilize the cavern or to check the design of the rock support intended to be used. By employing classic block theory and 3D block-cutting analysis *simultaneously* we can deal with more complicated issues and thus obtain more intensive and extensive knowledge of the block failure occurring in the fractured rock mass.

2. Identification of removable and key blocks

We use block theory and 3D block-cutting analysis to study the stability of an underground oil-storage cavern in China and the effectiveness of the support measures used in the rock mass surrounding the cavern. The cavern was constructed in a granitic gneiss region and is

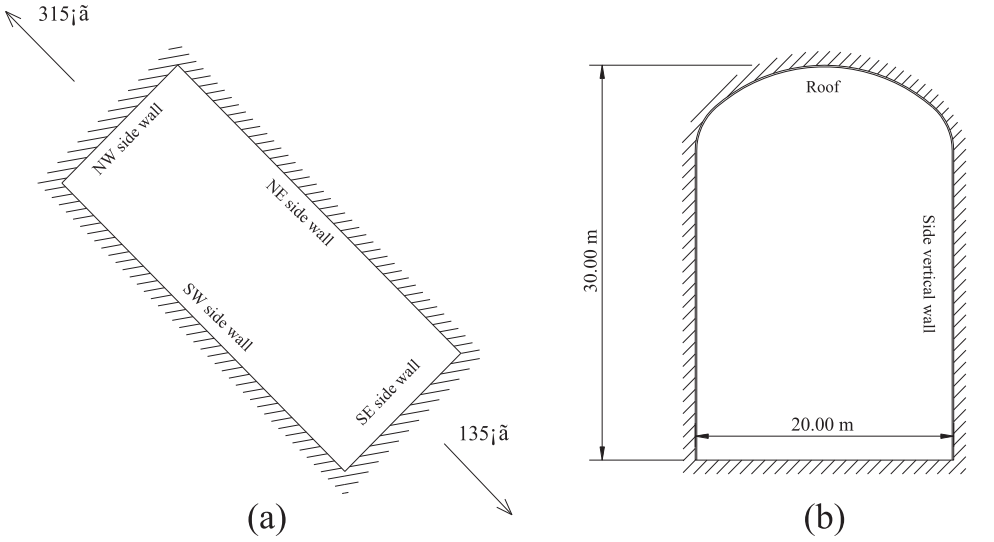

Fig. 1. Sketches showing: (a) the orientation, and (b) cross-section of the cavern.

Table 2
The geometrical parameters of the joint sets.

Joint set	Orientation	Friction angle (°)
1	70°∠75°	31
2	85.5°∠78.5°	31
3	112°∠56°	31
4	139.5°∠79.5°	31

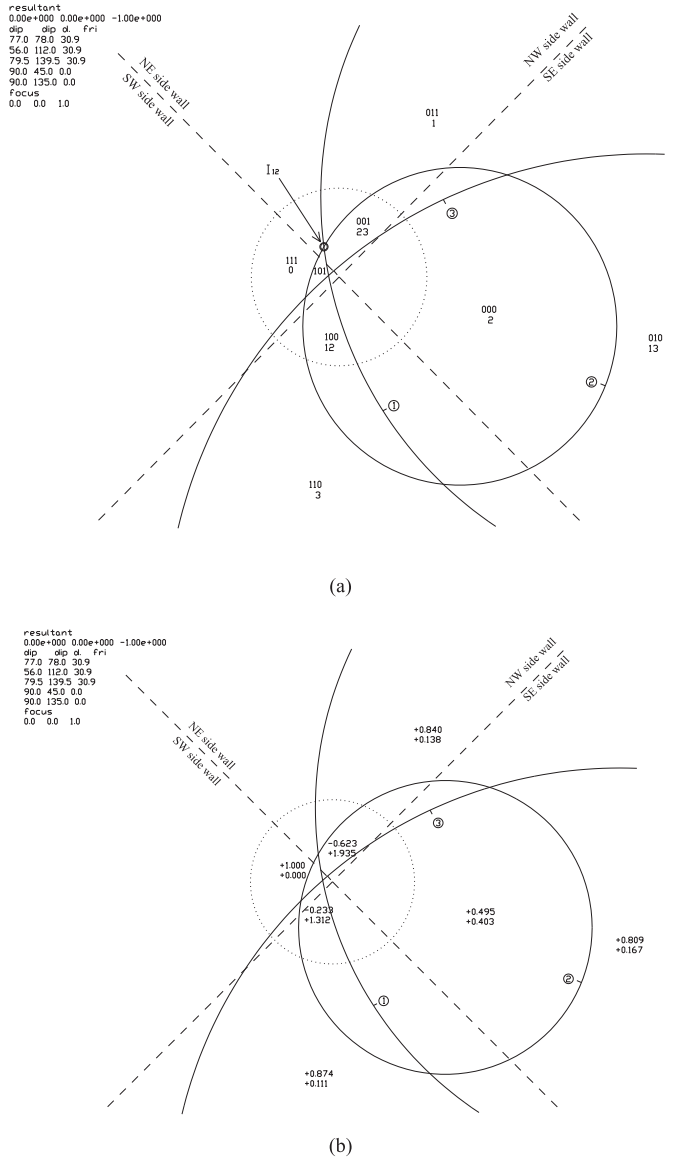

Fig. 2. Stereographic projections showing: (a) the joint pyramid and failure mode, and (b) residual sliding force and stability factor (ignoring cohesion).

arch-shaped (with a height of 30 m and span of 20 m), as shown in Fig. 1. The orientation of the cavern is NW315°. The rock mass is hard and contains a large number of joints. Failure of this kind of rock mass is controlled by the features of the developed fractures and manifests itself as local failure of the blocks.

There are four main sets of joints in the cavern region and their geometrical parameters, as determined via an in situ investigation, are shown in Table 2. Different combinations of joint sets may form different joint pyramids (JPs) and key blocks in different surface(s) of the excavation. The orientations of joint sets 1 and 2 are so similar that they can be averaged and treated as one joint set. Using the resulting 3 joint sets, we created the stereographic projections shown in Fig. 2.

In Fig. 2, the solid circles denote the projections of the joints and the dashed lines denote those of the excavation surfaces of the cavern. As the side walls of the cavern are vertical, their projections are straight lines. In Fig. 2(a), the labels '101', '001', etc., are the JP codes and denote the projection regions of the corresponding JPs. The labels '2', '12', etc. below the JP codes, are the failure modes of the corresponding JP according to the given resultant forces. (In this analysis, only the force of gravity is considered; it is shown in the top-left corner of the figure and labeled 'resultant'.) A label '2' indicates that the sliding mode of the corresponding JP is single-face sliding along face 2. Similarly, '12' indicates that the sliding mode is double-face sliding along faces 1 and 2.

In Fig. 2(b), the label '0.495' corresponds to the residual sliding force on the unit volume of the corresponding JP (JP 000). As cohesion at the sliding face is ignored when determining the sliding mode, the calculated residual sliding force on unit volume is not dependent on the volume of the JP or block and is dimensionless. Hence, we can obtain the residual sliding force on unit volume. The label '0.403' (below the previous label) denotes the stability factor of JP 000. This is also independent of the volume of the JP or block when cohesion is ignored.

The removability theorem of block theory states that if a JP (which is not empty and occupies a finite region, as in Fig. 2) is entirely contained inside a space pyramid (SP), then the corresponding block formed by the intersection of the JP and EP (EP = ~SP) is removable. Moreover, when the residual sliding force is positive, i.e. the sliding force is great than the frictional resistance in the sliding direction, this JP can form a key block. In this work, as cohesion at the sliding face is not considered, our results tend to be conservative and safe. Hence, it is impossible for our analysis to omit a key block (of course, we also need to remember that we do not consider other aspects of the system such as cracking and rotation of the rock blocks due to the assumptions inherent in block theory). Table 3 gives the results of the analysis of removable and key blocks in relation to the different excavation surfaces.

3. Analysis of block morphology and definition of a support-required block

For a given type of key block, there is a maximum block size beyond which blocks cannot be removed (the 'maximum key block' is formed when the extensions of the fractures are infinite and the fracture spacing is very small compared to the definite size of the cavern). Such a block requires the largest supporting force. As the actual spacing of fractures is not so small in practice and their extensions are finite, the concept of a maximum block is too conservative to apply in support analysis.

However, we can analyze the shape of the maximum block to identify which of the key blocks require support (i.e. are 'support-required' blocks). Maximum blocks can be drawn corresponding to the data given in Table 3, as shown in Fig. 3. Table 3 indicates that the block formed by JP 100 and the NE side wall is stable. However, the other two are key blocks.

Theoretically, these key blocks are unstable. We therefore need to investigate their morphologies and stabilities in order to decide what rock support measures are required. We note, however, that some key blocks do not need to be specifically considered in the subsequent analysis due to their 'special' morphologies. We can decide if this is the

Table 3
Removable blocks and key blocks (marked with an asterisk).

Location	Joint pyramid
NE side wall	100
SW side wall	011*
Roof	010*

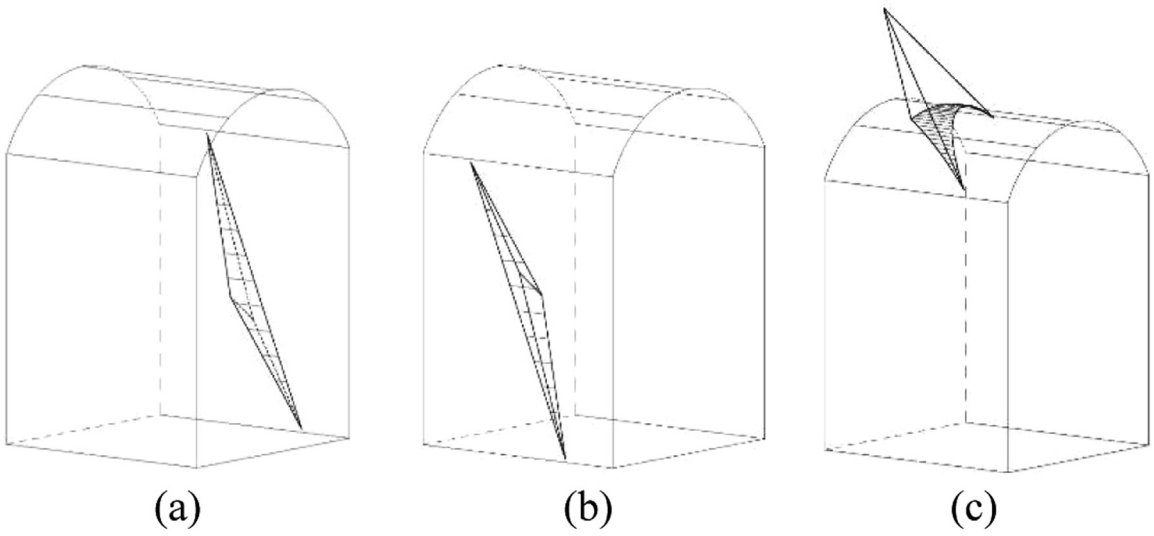

Fig. 3. The maximum blocks in the cavern formed by the excavation surface and (a) JP 100, (b) JP 011, and (c) JP 010.

case by drawing and analyzing the morphology of the block. Consider the block shown in Fig. 3(b). This key block is slender and clings to the excavation surface. Its depth beneath the excavation surface is shallow and its volume is small. It would probably drop after excavation, but normal reinforcement measures are likely to be sufficient to ensure its stability. Hence, we do not need to consider this block in subsequent rock support analysis.

The reason why this key block is slender and clings to the excavation surface can be discovered from the stereographic projection in Fig. 2(a). We all know that an intersection line between two fracture planes is projected to be a point in a stereographic projection. Thus, I_{12} denotes the point which is the projection of the intersection line between joint sets 1 and 2. From Fig. 2(a) we can find that I_{12} is adjacent to the straight line corresponding to the projection of the SW vertical side wall, which means that the orientation of the intersection line is approximately that of the SW side wall. Hence, the key block formed by JP 011 and the SW side wall has a slender shape.

After excluding key blocks that do not need to be considered further, the rest of the key blocks constitute the support-required blocks. In the present case, we can see that the only support-required block is JP 010.

4. Advantages of 3D block-cutting analysis

One advantage of 3D block-cutting analysis[8–14] is that it can be used to identify all the blocks formed by fractures of finite size in a given rock mass domain. The process therefore reveals the blocks located inside the rock mass in addition to those exposed on the excavation surfaces. The blocks may be composed of dozens or hundreds of faces with convex or concave shapes. Fig. 4 illustrates the sort of results typically obtained using 3D block-cutting analysis.

Block-cutting analysis undoubtedly constitutes an important progression in block theory and potentially has a wide range of applications in fractured rock mass research. Using the technique, we can directly obtain the shape, volume, and development features of the blocks present. Thus, we can analyze how these quantities vary for different DFNs. As the presence of fractures is the most important characteristic of the rock mass (and the origin of its anisotropy), we can carry out various studies by means of block-cutting analysis. These include (but are not limited to):

(1) Analyzing the existence of blocks cut by fractures with specific orientations, spacings, and extensions. If the spacings are large, and the extensions small enough, it is probable that the fractures cannot form closed blocks.
(2) Analyzing the progressive failure of the block system. This application will be discussed below in more detail.
(3) Quantitatively assessing the degree of block development and integrity of the rock mass. According to Ref.,[17] the larger the ratio of trace length to spacing, the greater the degree of development of the rock mass and the lower its integrity. When the aforementioned ratio is 3–4, the fractures split the rock mass into relatively 'blocky' discrete aggregates. Hence, the ratio of trace length to spacing is the most important factor to derive when assessing the degree of block development and integrity of the rock mass.
(4) Analyzing the connectivity of fracture networks. Connectivity is a core parameter in many fracture-related topics, e.g. synthetic evaluation of the shear strength of a sliding plane simultaneously passing through a number of fractures and blocks.
(5) Identifying fractures that are connected and form a pathway for flow when analyzing fluid flow in fractured rock masses. It has been proposed that the boundaries of all the enclosed blocks identified by 3D block-cutting analysis form flow pathways.[18] The boundaries of the blocks are composed of the 'loops' that are formed by the intersecting lines between all the faces (fractures and other surfaces). Therefore, the connection relationship between fractures can be determined according to the linkages between loops. Accordingly, the linkages of the nodes (as used in finite-element analysis) between different faces can also be determined.
(6) Generating computational meshes for 3D discontinuous deformation analysis and numerical manifold method.[19]

5. Progressive failure analysis

Block theory is capable of identifying removable and key blocks by use of the finiteness and removability theorems. The blocks which can be investigated in classic block theory are only those located on the excavation surfaces. However, we often need to consider an important problem: Are the inner blocks going to be stable when a surface block collapses? If the inner blocks are also going to collapse, how will they do so and how far will this progressive collapse continue? To address these questions, we need to perform a progressive block failure analysis.[8,11–13,15,16]

When a surface block collapses, the constraints it places on its adjacent inner blocks will vanish. Thus, the inner blocks become surface blocks and may also fail. The process of progressive failure may therefore continue indefinitely. After executing a 3D block-cutting analysis, we know the topological structures and the geometric relationships between all the blocks. Therefore, it is possible to analyze

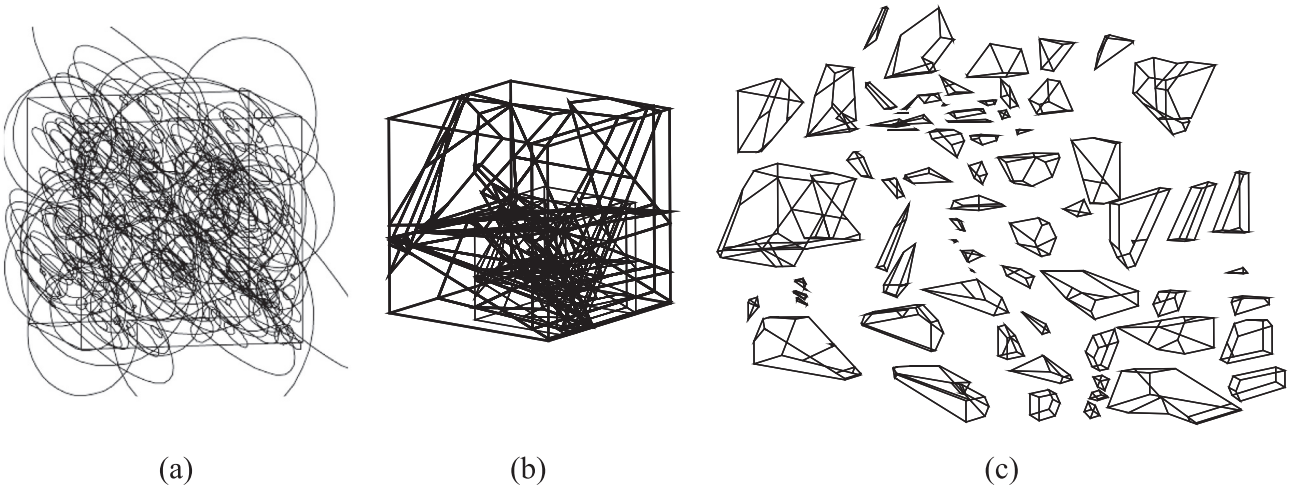

Fig. 4. Blocks cut by a stochastic fracture network showing: (a) the 3D DFN, (b) blocks assembled together within the domain of interest, and (c) the blocks separated from one another.

the blocks to look for signs of impending progressive failure. Three types of translational failure modes feature in block theory: single-face sliding, double-face sliding, and lifting.[1] Using certain rules to judge the likelihood of these failure modes occurring, we can successfully analyze the progressive failure of blocks.

If a block B slides along one of its faces, its direction of movement $\hat{s}$ is parallel to only one fracture face, such as face i:

$$\hat{s} = \hat{s}_i = \frac{(\hat{n}_i \times \vec{r}) \times \hat{n}_i}{|\hat{n}_i \times \vec{r}|} \tag{1}$$

where $\vec{r}$ is the active resultant, $\hat{n}_i$ is the upward normal vector to face i, and $\hat{s}_i$ is the orthographic projection of $\vec{r}$ on face i.

Two conditions have to be satisfied for block B to slide along face i. The first is that the active resultant makes the block contact with face i:

$$\vec{r} \cdot \hat{v}_i \le 0. \tag{2}$$

where $\hat{v}_i$ is the unit vector normal to face i, directed into the block. The second is that the active resultant makes the block move away from the other fracture faces:

$$\hat{s} \cdot \hat{v}_k > 0 \text{ for all } k, \quad k \ne i. \tag{3}$$

If Eq. (3) was written in the form $\hat{s} \cdot \hat{v}_k \ge 0$, then a block having a fracture face parallel to the sliding face i is not excluded. This means that the block will fail in the single-face sliding mode. Considering that the actual faces of fractures are not planar but fluctuate, the sliding of these kinds of block can be easily hindered by a small amount of surface fluctuation. Hence, it is reasonable to exclude these kinds of block.

If block B slides along two nonparallel faces i and j simultaneously, the sliding direction $\hat{s}$ is parallel to the intersection line of faces i and j:

$$\hat{s} = \hat{s}_{ij} = \frac{\hat{n}_i \times \hat{n}_j}{|\hat{n}_i \times \hat{n}_j|} \text{sign}[(\hat{n}_i \times \hat{n}_j) \cdot \vec{r}] \tag{4}$$

where sign$[x]$ is equal to – 1, 0, or 1 when x is < 0, $= 0$, or > 0, respectively. The active resultant must keep the block in contact with faces i and j, and depart from the other fracture faces. Thus, the following conditions must exist for sliding along faces i and j:

$$\hat{s}_i \cdot \hat{v}_j \le 0, \tag{5}$$

$$\hat{s}_j \cdot \hat{v}_i \le 0, \tag{6}$$

$$\hat{s} \cdot \hat{v}_k > 0 \text{ for all } k, \quad k \ne i \text{ or } j. \tag{7}$$

(Again, if Eq. (7) was $\hat{s} \cdot \hat{v}_k \ge 0$, then a block having fracture faces parallel to the sliding faces cannot be excluded and the block can fail in the double-face sliding mode.)

If block B is lifting, the direction of motion $\hat{s}$ is parallel to the direction of the active resultant $\vec{r}$:

$$\hat{s} = \frac{\vec{r}}{|\vec{r}|} = \hat{r}. \tag{8}$$

The active resultant $\vec{r}$ makes the block translate freely from its home, so that the block's motion is not hindered by any of the fracture faces:

$$\hat{r} \cdot \hat{v}_k > 0. \tag{9}$$

These rules have to be satisfied if the corresponding failure mode is to happen, regardless of whether the block is convex or concave. Fig. 5 illustrates the single-face sliding of a concave block in a 2D section. In Fig. 5(a), the block has two parallel sliding faces, and the sliding direction is $\hat{s}_1 (= \hat{s}_2)$. In Fig. 5(b), the sliding direction is $\hat{s}_2$, because Eqs.

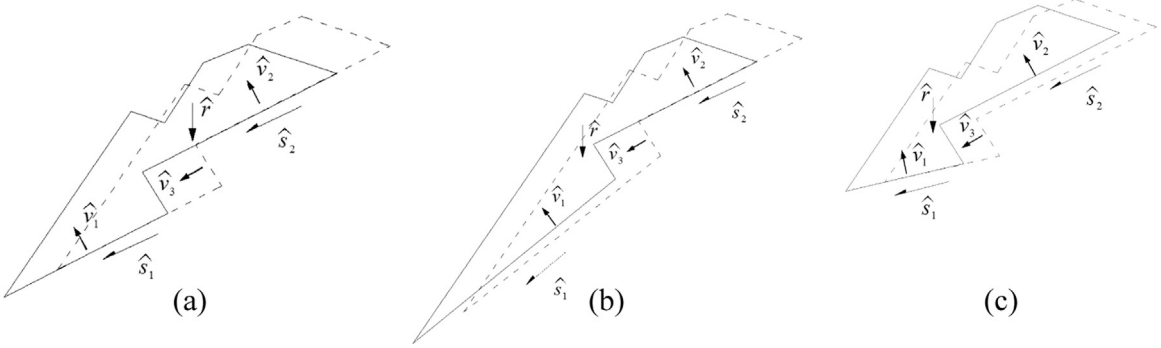

Fig. 5. Single-face sliding examples for concave blocks. (a) The sliding direction is $\hat{s}_1 (= \hat{s}_2)$ because planes P_1 and P_2 are parallel. (b) The sliding direction is $\hat{s}_2$. P_1 and P_3 are becoming open. (3) The sliding direction is $\hat{s}_1$, and P_2 and P_3 are becoming open.

(1)–(3) can be satisfied only when the block slides along plane P_2 (which corresponds to $\hat{v}_2$ in the figure). It is impossible for the sliding direction to be $\hat{s}_1$ (if it were, then $\hat{s}_1 \cdot \hat{v}_2 < 0$ and the block will invade the rock mass surrounding P_2). In Fig. 5(c), the sliding direction is $\hat{s}_1$, and P_2 and P_3 are opening up.

It is a simple matter to program a computer to carry out the judgment process. Identification of single-face sliding, and cycling the analysis to search for failure blocks in batches, can be fulfilled using the following pseudo-code.

```
Begin:
  ……
ln_00;
  for each block j = 1 to m do      /* there are m blocks obtained
                                    by 3D block-cutting analysis */
  count the fracture faces of block /* count the number of the
   j;                               fracture faces, which may
                                    become
                                    free surfaces when the adjacent
                                    blocks fail   */
  for each fracture face i = 1 to n /* there are n fracture faces in
   do                               block j. n may change   */
  calculate ŝ_i;
  a_1 = r⃗·v̂_i;
  if (a_1 > 0.0001) goto ln_02;     /* go to the next fracture face
                                    of block j   */
  for each fracture face k = 1 to n
   do
  if (k = i) goto ln_01;
  a_2 = ŝ·v̂_k;
  if (a_2 < −0.0001) goto ln_02;
ln_01;
  enddo                             /* k */
  write: 'Block', j, ' slides along
   face ', i;
  goto ln_03;                       /* go to the next block   */
ln_02;
  enddo                             /* i */
  analyze the double-face sliding
   mode;
  analyze the lifting mode;
ln_03;
  change all the fracture faces of
   adjacent blocks of block j into
   free surfaces;
  enddo                             /* j */
  if (there are progressive failure
   blocks newly searched) goto
   ln_00;
                                    /* return to search the next
                                    batches of failure blocks   */
  ……
end
```

According to the principles of the three failure modes, progressive failure blocks are potentially key blocks. When the fractures in the rock mass reduce its shear strength to a significant degree, these blocks may not be self-stabilized and may, instead, become key blocks. We may investigate the spatial range of progressive failure blocks *statistically* by performing dozens of simulations. If the rock support to be employed is subsequently designed in accordance with the range of progressive failure blocks derived, we can then ensure the stability of the whole block system.

6. Application of progressive failure analysis

We first need to carry out some 3D DFN modeling[2,6,20] before performing the block-cutting analysis. Monte-Carlo simulations are performed according to the given probability distributions for the fractures' geometric parameters. As a result, each fracture can be specified by a set of parameters including the dip direction, dip angle, radius, and coordinates of the disk's center (a circular disk shape is the one most often used in fracture network modeling for the sake of simplicity). In our Monte-Carlo simulations, the orientations of the joints are assumed to be constant (this is because stochastically changing the orientations around their averages does not notably affect the results of the analysis). Therefore, we do not need to consider an orientation probability distribution. The probability distributions for the trace length and spacing are assumed to have negative exponential forms (this is the form of distribution that is most commonly used for these two quantities[20–22]). Only one parameter is employed in the distributions (i.e. the means) and the locations of the joints obey a uniform distribution in space.

The geometric parameters usually have distributions that vary in different parts of the cavern due to the random way in which fractures occur. A typical part of the cavern was chosen and studied. The variation in the geometrical parameters observed for the fractures within this part is definite, as shown in Table 4. We can use these parameters to generate a DFN using Monte-Carlo simulation. After the DFN is generated, we can obtain a trace map of the fractures in a given section, as shown in Fig. 6. The trace map is drawn by judging whether or not each fracture disk intersects with the section. If it does, then it forms a trace in the section.

According to Ref.,[17] the larger the trace length to spacing ratio, the higher the degree of development of the rock mass and the lower is its integrity. Hence, this ratio is a very important parameter. We shall use this parameter to investigate, statistically, how the progressive failure of the blocks changes as the characteristics of the development of fractures change. We consider two scenarios.

6.1. Large trace length to spacing ratio

We first consider the situation in which the ratio takes on the largest value expected from the range of the parameter values shown in Table 4. Thus, we take the mean trace length to be 5.0 m and the mean spacing to be 1.0 m, so that the ratio is 5.0.

As DFNs are simulated stochastically, different simulations yield different results. One sample of closed blocks identified (within a certain domain of the rock mass) is shown in Fig. 7. There are 5492 closed blocks shown. Unlike in Ref.[11] which used some specific cutting planes, the simulated rock mass domain surrounding the underground chamber in our algorithm is defined by several coordinate values. If a vertex of a block is located *outside* the simulation domain (i.e. its coordinates exceed the allowed range of coordinate values), that block is not considered to be enclosed within the simulation domain and so cannot be identified. In other words, only those blocks that are wholly located within the simulation domain are identified and illustrated. Blocks that are located simultaneously inside and outside the simulation domain are not shown. Of course, provided the chosen domain is big enough, all

Table 4
Geometrical parameters of the fractures in the DFN simulations.

Joint set	Orientation (°)	Mean trace length (m)	Mean spacing (m)
J1	78∠77°	2–5	1–2
J2	112∠56°	2–5	1–2
J3	139.5°∠79.5°	2–5	1–2
Deterministic fissures	Input directly into the simulation according to the measured position, orientation, and extension data.		

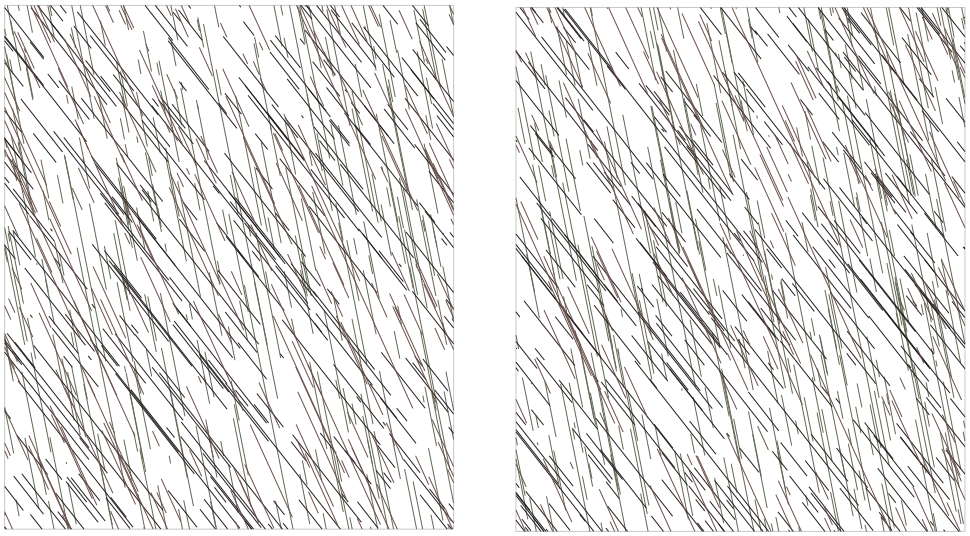

Fig. 6. Trace maps corresponding to a mean trace length of 3 m and spacing of 1.2 m. The figures are 50 m in height and 40 m in width.

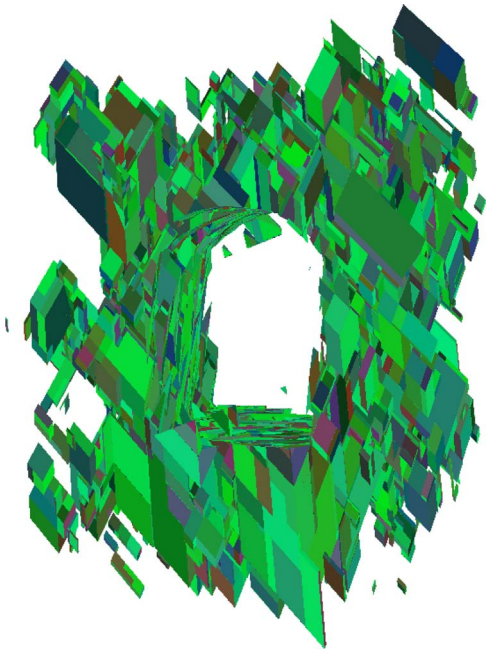

Fig. 7. The closed blocks identified in a certain domain of the rock mass (sample 1).

the blocks that are close to the excavation surfaces of the underground chamber will be found and the progressive block failure analysis will not be affected by this treatment.

The progressive failure of the blocks shown in Fig. 7 can now be investigated, as shown in Fig. 8. The blocks failing are divided into batches. The first batch of failure blocks (i.e. those that would collapse) are located on the surfaces of the cavern. Then, if collapse occurred, the inner blocks that are adjacent to the first batch of failure blocks become exposed and may also collapse. Hence, the second batch of failure blocks can be identified. By continuing the analysis in this manner, we can identify the way in which the failure of the blocks progresses. In all, seven batches of failure blocks were identified in the example shown. The number and volumes of the failure blocks are shown in Table 5 on a batch-by-batch basis. In this particular example, the total volume of the failure blocks from the second batch is much larger than that from the first batch. If a progressive failure analysis had not been carried out, all of the blocks liable to fail due to progressive failure would not have come to light (only the first batch would be known to us). This would threaten the stability of the cavern. Hence, progressive failure analysis is a very important tool.

The analysis results obtained for the other samples are shown in Figs. 9 and 10. The figures show that most of the failure blocks are small. This is because the smaller the block, the easier it is formed. At the same time, most of the failure blocks are close to the excavation surfaces, because these kinds of blocks are the ones most readily formed.

Each corner of a progressive failure block lies at a certain depth inside the rock mass measured from the excavation surface. The depth of the corner which is furthest from the surface is called the 'embedding depth'. This parameter is used to determine the length of rock bolts required. Figs. 8–10 show that the locations and volumes of the blocks are different in different simulation samples. However, the development degree and embedding depth of the blocks are statistically similar, on the whole. The distribution of the embedding depths of the blocks for several sets of simulations is shown in Fig. 11. The figure also reveals that most of the failure blocks have embedding depths that are small. However, a small portion of the blocks have embedding depths that are large. These blocks, although few in number, are of great importance in the subsequent support analysis.

For each simulation, we can obtain estimates of the mean and standard deviation of the embedding depths of the failure blocks (Table 6). For all of the estimates of the mean we can also obtain their mean, standard deviation, and coefficients of variation (ratio of standard deviation to mean) for a number of simulations, as we also show in Table 6. Similarly, we can also analyze the estimates of the standard deviation. The means of the embedding depths are close among the various simulation samples, with the coefficient of variation being 15.69%. The standard deviations of the embedding depths are also close, with the coefficient of variation being 15.36%.

Negative exponential functions are suitable for describing the distributions shown in Fig. 11. Using the mean of the estimates of the means given in Table 6, we can formulate the probability density function for the embedding depth:

$$f(x) = \frac{1}{0.7175}\exp(-x/0.7175). \tag{10}$$

The probability that the embedding depth is greater than x is

$$F(x) = \exp(-x/0.7175). \tag{11}$$

Hence, when the embedding depth of the failure block is greater than 3, 4, and 5 m, the probability of the block failing is 1.53%, 0.38%, and 0.09%, respectively. Therefore, if the acceptable probability of failure is 1.53% (or 0.38%) and the length by which the rock bolt should exceed the embedding depth is 1.0 m, then the length of the rock

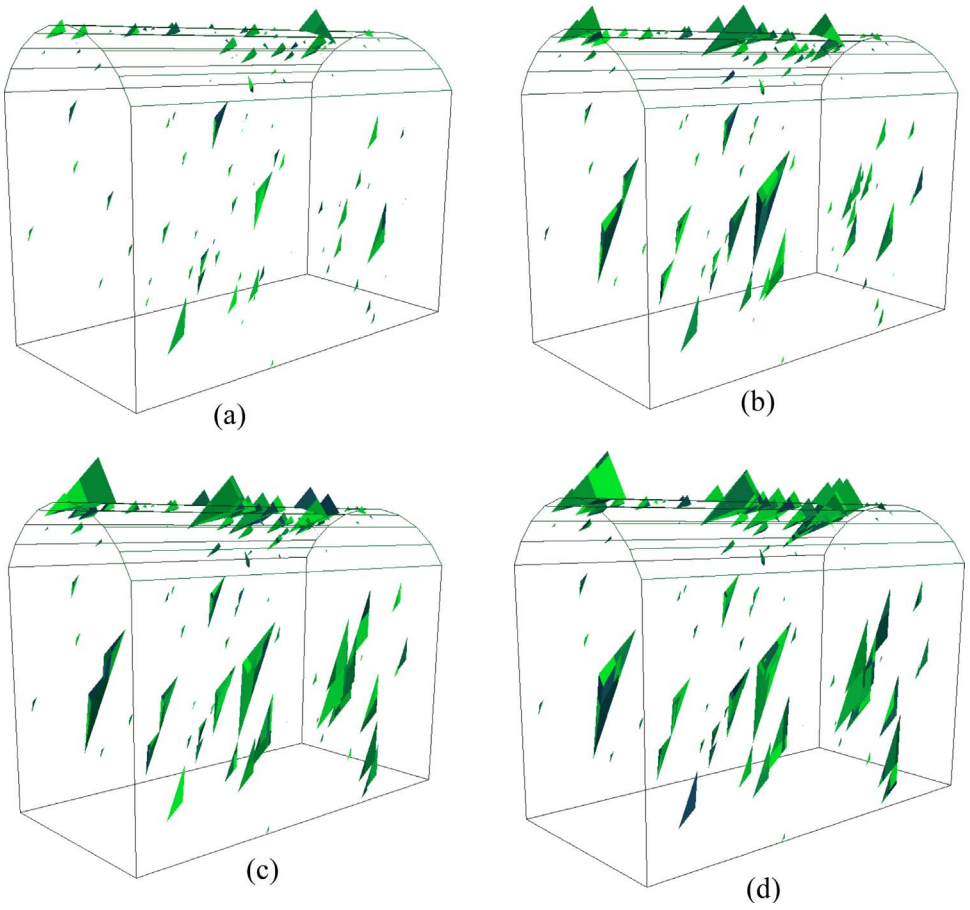

Fig. 8. The progressive failure blocks corresponding to Fig. 7 shown accumulatively. The progression of figures show the failure blocks: (a) from the first batch, (b) from the first two batches, (c) from the first three batches, and (d) from all the seven batches.

Table 5
The number and volumes of the failure blocks identified.

Batch no.	Number of blocks	Volume of blocks (m^3)
1	148	6.0424
2	79	21.0711
3	38	22.0089
4	9	7.1307
5	1	3.5509
6	1	0.8554
7	1	4.2032

bolt should be 4 m (or 5 m).

We can also find that the number of progressive failure blocks located on the roof is larger than the number located on the side walls of the cavern. The characteristics of the shapes of the blocks on the roof and the side walls are similar to those in Fig. 3. Given the former results we can conclude that more attention should be paid to the roof during rock support design.

6.2. Small trace length to spacing ratio

We next consider the situation in which the trace length is 5.0 m and the spacing is 2.0 m, so that the trace length to spacing ratio is 2.5.

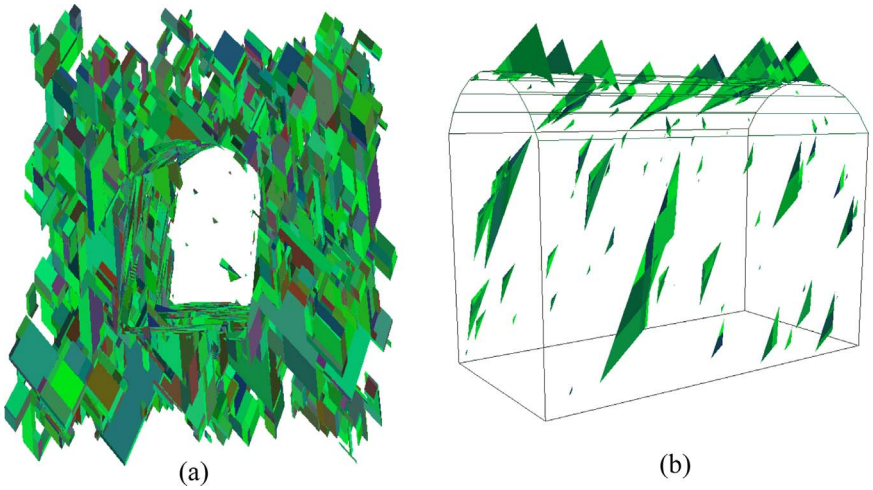

Fig. 9. The results for sample 2, showing: (a) the closed blocks, and (b) all the progressive failure blocks.

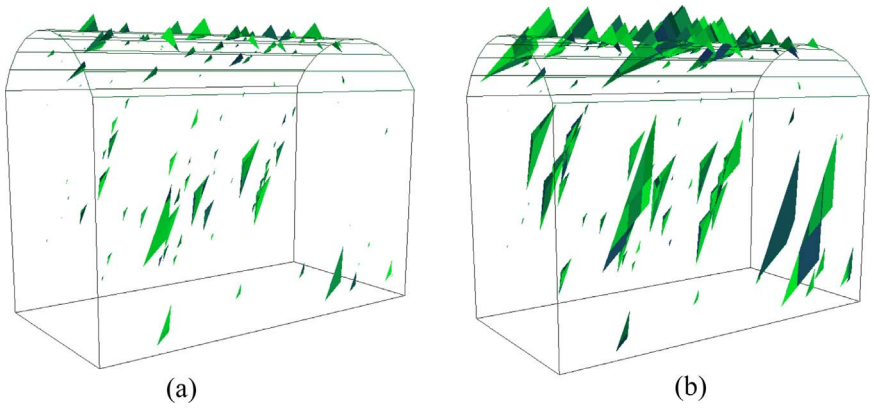

Fig. 10. The results for sample 3, showing: (a) the failure blocks from the first batch, and (b) all the progressive failure blocks.

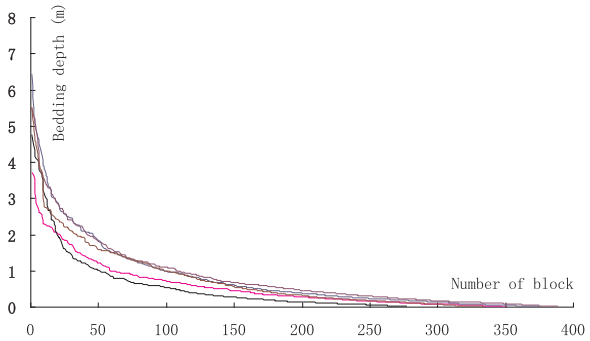

Fig. 11. Distribution of the embedding depths in various simulations.

Table 6
Estimates of the statistical parameters for the embedding depth in various simulations.

Sample no.	Estimated mean (m)	Estimated standard deviation (m)
1	0.5937	0.6568
2	0.6314	0.8530
3	0.8150	1.0031
4	0.8288	0.9451
5	0.8080	0.9054
6	0.8096	0.8999
7	0.5539	0.6424
8	0.6889	0.8224
9	0.6111	0.7006
10	0.8350	0.9445
Mean of all samples (m):	0.7175	0.8373
Standard deviation of all samples (m):	0.1126	0.1286
Coefficient of variation	15.69%	15.36%

In this case, the rock mass will not be fully cut and the rock mass is much more continuous, according to the results presented in Ref.[17] The results obtained in one particular simulation are shown in Fig. 12 and those for another in Fig. 13.

6.3. Block development and support analysis

After carrying out a large number of simulations, we have found the following statistical laws governing the distribution of progressive failure blocks:

(1) The failure blocks in the simulations do not just lie on the surface, nor do they extend over a very large range. Instead, they always extend, approximately, to a certain embedding depth beneath the surfaces of the cavern. (This corresponds to the quantitative results given above which showed that the mean embedding depths from the different simulations are close to one another.)
(2) The progressive failure blocks on the roof are more developed than those on the side walls of the cavern. The blocks on the side walls are formed by steep fractures. Hence they have slender shapes, and embedding depths that are shallow. So, the problem of block instability is less important for the side walls. Thus, less attention needs to be given to them during rock support analysis. This suggestion is in accordance with the results of previous analyses in Section 3.

The rock support design diagram for a typical cavern section is shown in Fig. 14. Two kinds of rock bolt are involved. Both are 25 mm in diameter but their lengths are different (the longer ones are 6 m in length; the others are 4.5 m long). They are used on the cavern surfaces in a 'criss-cross' pattern with spacings of 1.5 m × 3.0 m. In addition, the surfaces are reinforced using steel fiber shotcrete applied to a thickness of 0.12 m.

In the interest of safety, we take the analysis results obtained using a large trace length to spacing ratio as the reference to analyze the level of support required. Thus, according to the results above, we can expect that only 1.53% and 0.38% of the blocks may fail that if the rock bolts used are longer than 4 and 5 m, respectively.

On the whole, the lengths of the bolts shown in Fig. 14 exceed the embedding depths expected of blocks likely to undergo progressive failure. Considering that the shapes of the blocks are slender, which favors block stability, we can conclude that the rock support design suggested is capable of ensuring the stability of the cavern.

Of course, if the characteristics of the fracture development in other parts of the cavern are substantially different from those shown in Table 4 (i.e. the orientations, spacings, and trace lengths are significantly different), then it will be necessary to redo the analysis in order to ensure the stability of the rocks.

7. Conclusions

In this paper, we compare the application of block theory and 3D block-cutting analysis. We analyze the shortcomings of classic block theory and point out the advantages of both 3D block-cutting analysis and progressive block failure analysis. If we can use both of these methods properly (according to their different principles and scope of application), we can deal with more complicated issues and obtain a much better understanding of the applications studied. Our main conclusions are:

(1) Stereographic projections can be used to determine the removable and key blocks associated with the different excavation surfaces in the cavern. These results lay the foundation for further analysis of the morphologies of the blocks, their stability, and the support measures required.

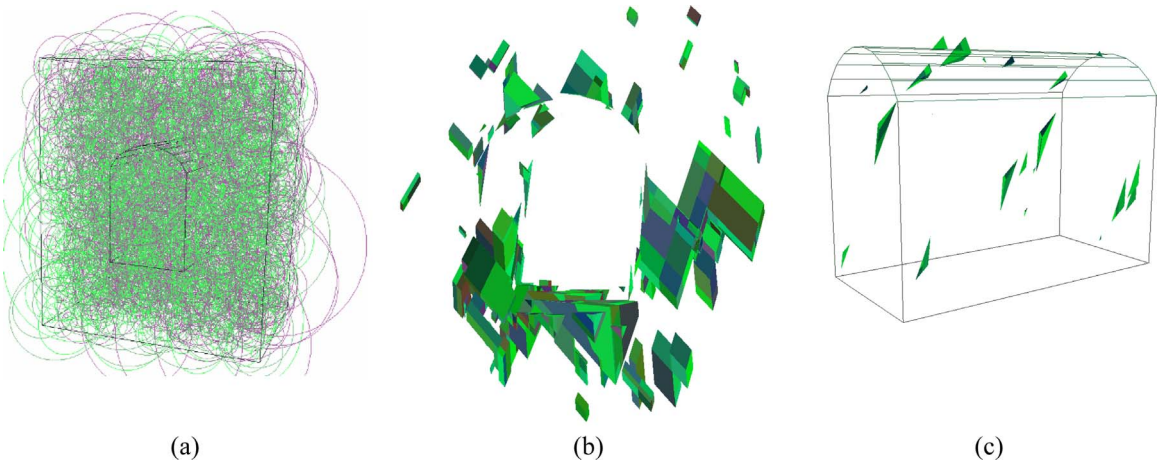

Fig. 12. Example simulation results showing: (a) the DFN, (b) the closed blocks within the domain of simulation, and (c) the progressive failure blocks.

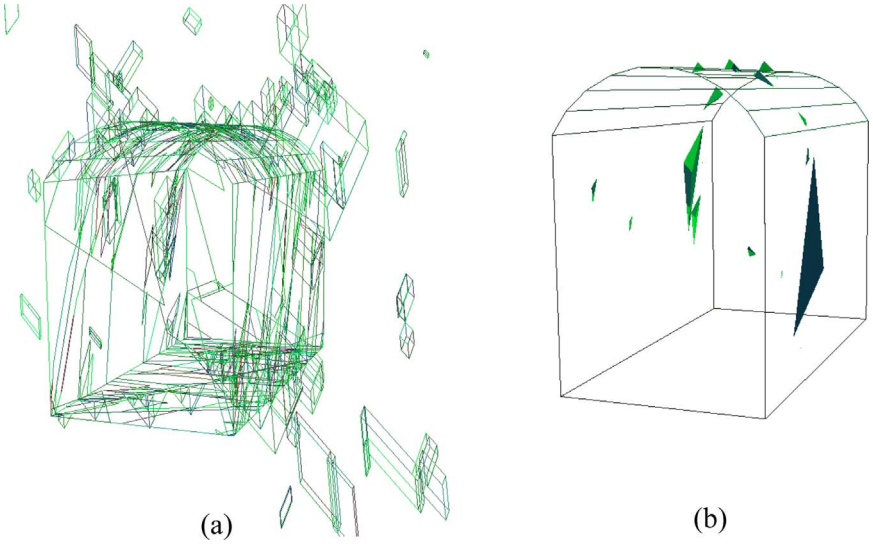

Fig. 13. Results of another simulation showing: (a) the closed blocks within the domain of simulation, and (b) the progressive failure blocks.

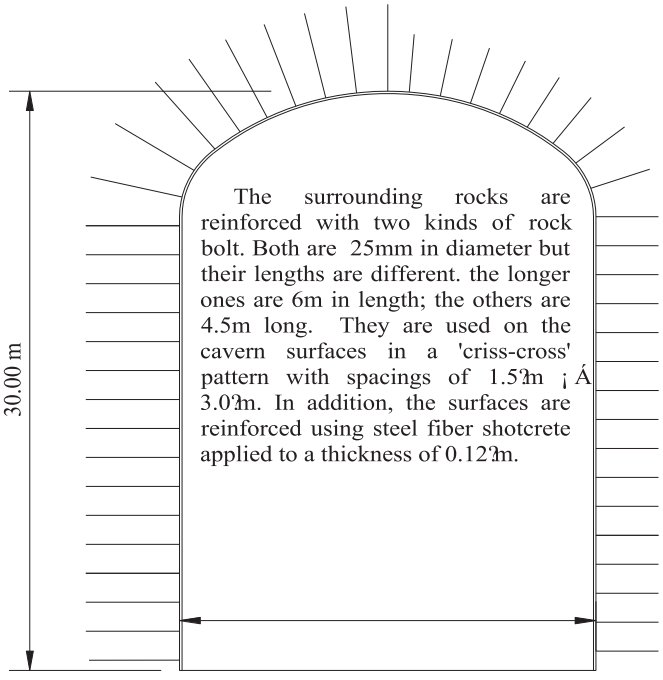

Fig. 14. A diagram showing the reinforcements typically used in a cavern.

(2) The concept of a 'support-required' block is very useful (defined as one of the key blocks that remain after excluding those which are slender and either cling to the excavation surface or penetrate deep into the rock mass). Actually, such slender key blocks do not need to be specifically involved in the rock support analysis. This is because their depths beneath the excavation surfaces are very shallow, or because the roughness of the fractures can prevent them from failing. By drawing and analyzing the shapes of the maximum blocks (which are those likely to be formed when the fractures are extended indefinitely in a definite-sized cavern), we can identify the support-required blocks from the key blocks.

(3) All the spatial blocks formed by fractures of finite size can be identified using 3D block-cutting analysis. The blocks can be of any shape and their locations in the 3D space can be determined for a certain DFN simulated. This approach makes up for the shortcomings of classic block theory by determining the blocks which are cut by a large number of fractures with finite sizes and certain positions (each fracture has a certain position in a DFN, even if the DFN is generated via Monte-Carlo simulation). The degree of development of the blocks and the integrity of the rock mass can also be analyzed.

(4) Based on the results of the 3D block-cutting analysis, the progressive failure of the block system can be analyzed by referring to the appropriate criteria for the various failure modes encountered in block theory. In this way, we found that the development degree

and mean embedding depth of the progressive failure blocks are statistically similar, on the whole (even though the locations and volumes of the blocks are different in different simulations). This discovery is very useful for the analysis of rock block support. The results of the analysis indicate that the problem of block stability is not critical and that the rock support design can ensure the stability of the rocks surrounding the cavern.

Acknowledgments

This research was sponsored by the General Program of National Natural Science Foundation of China (Grant no. 51679012) and the Key Program of National Natural Science Foundation of China (Grant no. 51539002).

References

1. Goodman RE, Shi GH. *Block Theory and its Application to Rock Engineering.* Englewood Cliffs, New Jersey: Prentice-Hall Inc; 1985.
2. Shi GH, Goodman RE. The key blocks of unrolled joint traces in developed maps of tunnel walls. *Int J. Numer. Anal Methods Geomech.* 1989;13:131–158.
3. Shapiro A, Delport JL. Statistical analysis of jointed rock data. *Int J Rock Mech Min Sci.* 1991;28(5):375–382.
4. Hatzor Y, Feintuch A. The joint intersection probability. *Int J Rock Mech Min Sci.* 2005;42(4):531–541.
5. Zhang QH, Wu AQ, Zhang LJ. Statistical analysis of stochastic block and its application to rock support. *Tunn Undergr Space Technol.* 2014;43:426–439.
6. Zhang QH. *Fundamental Research on Application of Rock Mass Block Theory*. Wuhan: Hubei Science and Technology Press; 2010 [in Chinese].
7. Zhang Q-H. Block-dividing limit equilibrium analysis method with multiple sliding-planes. *Chin J Rock Mech Eng.* 2007;26(8):1625–1632 [in Chinese].
8. Lin D, Fairhurst C. Static analysis of the stability of three-dimensional blocky systems around excavations in rock. *Int J Rock Mech Min Sci.* 1988;25(3):139–147.
9. Ikegawa Y, Hudson JA. A novel automatic identification system for three-dimensional multi-block systems. *Eng Comput.* 1992;9(2):169–179.
10. Jing L. Block system construction for three-dimensional discrete element models of fractured rocks. *Int J Rock Mech Min Sci.* 2000;37(4):645–659.
11. Shi GH. Producing joint polygons, cutting joint blocks and finding key blocks from general free surfaces. *Chin J Rock Mech Eng.* 2006;25(11):2161–2170.
12. Elmouttie M, Poropat G, Krähenbühl G. Polyhedral modelling of rock mass structure. *Int J Rock Mech Min Sci.* 2010;47(4):544–552.
13. Zhang QH. Advances in three-dimensional block cutting analysis and its applications. *Comput Geotech.* 2015;63:26–32.
14. Zheng Y, Xia L, Yu Q. A method for identifying three-dimensional rock blocks formed by curved fractures. *Comput Geotech.* 2015;65:1–11.
15. Wibowo JL. Consideration of secondary blocks in key-block analysis. *Int J Rock Mech Min Sci.* 1997;34:3–4 [paper No. 333].
16. Yarahmadi BAR, Verdel T. The key-group method. *Int J Numer Anal Met Geomech.* 2003;27(6):495–511.
17. Zhang Q-H, Bian Z-H, Yu M-W. Preliminary research on rockmass integrity using spatial block identification technique. *Chin J Rock Mech Eng.* 2009;28(3):507–515 [in Chinese].
18. Zhang Q-H, Yin J-M. Solution of two key issues in arbitrary three-dimensional discrete fracture network flow models. *J Hydrol.* 2014;514:281–296.
19. Zhang Q-H, Lin S-Z, Xie Z-Q, Su H-D. Fractured porous medium flow analysis using numerical manifold method with independent covers. *J Hydrol.* 2016;542:790–808.
20. Kulatilake PHSW, Wathugala DN, Stephansson O. Joint network modeling with a validation exercise in Stripa mine, Sweden. *Int J Rock Mech Min Sci.* 1993;30(5):503–526.
21. Hudson JA, Priest SD. Discontinuities and rock mass geometry. *Int J Rock Mech Min Sci.* 1979;16:339–362.
22. Kulatilake PHSW, Chen J, Teng J, et al. Discontinuity geometry characterization in a tunnel close to the proposed permanent shiplock area of the Three Gorges Dam Site in China. *Int J Rock Mech Min Sci.* 1996;33(3):255–277.